

## **Temperature development and cracking characteristics of high-strength concrete slab at early age**

\*Chung-Hao Wu<sup>1)</sup>, Yu-Feng Lin<sup>2)</sup>, Shu-Ken Lin<sup>3)</sup>, and Chung-Ho Huang<sup>4)</sup>

<sup>1), 2)</sup> *Department of Civil Engineering/Chienkuo Technology University  
No.1, Chiehshou North Road, Chungshau City 500, Taiwan*

<sup>1)</sup> [chw@ctu.edu.tw](mailto:chw@ctu.edu.tw)

<sup>2)</sup> [lyf@ctu.edu.tw](mailto:lyf@ctu.edu.tw)

### **ABSTRACT**

High-strength concrete (HSC) generally made with high amount of cement which may release large amount of hydration heat at early age. The hydration heat will increase the internal temperature of slab and may cause potential cracking. In this study, slab specimens with a dimension of 600 × 600 × 100 mm were cast with concrete incorporating silica fume for test. The thermistors were embedded in the slabs therein to investigate the interior temperature development. The test variables include water-to-binder ratio (0.25, 0.35, 0.40), the cement replacement ratio of silica fume (RSF; 5%, 10%, 15%) and fly ash (RFA; 10%, 20%, 30%). Test results show that reducing the W/B ratio of HSC will enhance the temperature of first heat peak by hydration. The increase of W/B decrease the appearance time of second heat peak, but increase the corresponding maximum temperature. Increase the RSF or decrease the RFA may decrease the appearance time of second heat peak and increase the maximum central temperature of slab. HSC slab with the range of W/B ratio of 0.25 to 0.40 may occur cracking within 4 hours after casting. Reducing W/B may lead to intensive cracking damage, such as more crack number, and larger crack width and length.

### **1. INTRODUCTION**

(Mehta 1986), (Zou et al. 2012) and (Chu et al. 2013) indicated that mixing cement with water causes a rapid evolution of heat that lasts for a few minutes, yielding the first peak. This represents the heat of the solution of aluminates and sulfates. This initial evolution of heat ceases quickly when the solubility of aluminates is depressed by the presence of sulfate in the solution. The next heat evolution cycle, culminating in the second heat peak after around 4 to 8 hours for most Portland cement, represents the

---

<sup>1)</sup> Assistant Professor

<sup>2)</sup> Associate Professor

<sup>3)</sup> Lecturer

<sup>4)</sup> Assistant Professor

heat of formation of ettringite. It is believed that the contributions to heat evolution at this period are dominated by  $C_3S$  and  $C_3A$  as presented by (Mindess 2002) and (Li et al. 2016). The paste of a properly retarded cement will retain much of its plasticity before the commencement of this heat cycle and will stiffen and begin to set before reaching the apex, which corresponds to the final set.

(ACI Committee 363 2010) shows that high-strength concrete (HSC) is defined as having a compressive strengths of higher than 40 MPa (6000 psi). Generally, the HSC has low water-to-binder ratio (W/B) and a high cement content. When it particularly incorporates silica fume in concrete, the heat of hydration at early age will be increased. This may increase the drying shrinkage deformation, leading to a potential cracking. (Bentz 2008) reported that increasing the amount of cement per cubic meter of concrete to 59 kg increased the temperature by up to 6~8 °C in HSC. A high cement content of around 600 kg/cm<sup>3</sup> without the inclusion of Pozzolan materials can increase the temperature to 60~80 °C, negatively affecting the volumetric stability of HSC. (Langan 2002), (Utsi 2012) and (Jiang et al. 2015) investigated that concrete incorporating with fly ash and silica fume can exhibit delayed hydration, reducing the heat of hydration, and a reduced rate of hydration reaction of the silica fume at early age because of the presence of fly ash. In addition, (Maria 2002) and (Yang et al. 2005) presented the rate of shrinkage of HSC that contains silica fume is increased by increasing the silica fume content at early age. However, when the wet curing period exceeds 7 days, the total rate of shrinkage of HSC will be similar to that of normal concrete.

(Holt et al. 2004) and (Yoo et al. 2014) researched that a slab cast with HSC typically has a relatively large exposed surface, enabling a rapid heat evaporation and a decline in the surface temperature, whereas the internal temperature persistently rise by hydration. Thus, the different temperature distributions may be induced inside the slab and form a thermal gradient which cause the development of tensile strength. When the tensile strength exceeds that of concrete at any point, unnoticeable internal cracks will occur. (Mindess et al. 2003) and (Wan et al. 2016) studied that cracking, in most instances, originates internally, forming a network of microcracks throughout the concrete. Internal damage may be considerable before cracks are visible at the external surface.

(Al-Fadhala et al. 2001) and (Mihashi et al. 2004) described that high quality mixing materials and effective curing are necessary to control the temperature deformation of HSC that contains silica fume at early age, but these are not the only important factors. The temperature of concrete in situ will vary with the humidity and environmental conditions. To prevent thermal cracking, as shown by (Huo 2006), (Park et al. 2015) and (Lin et al. 2012), concretes must be properly cured at the correct time. Consequently, this study explores to investigate the temperature development of an HSC slab that contains silica fume and fly ash at early age, using an especially designed temperature measurement system. The goal is that this work will contribute to a better understanding of HSC that contains silica fume at early age, and in particular to the determination of the specific point of heat generation from placement to steady temperature stage.

## **2. EXPERIMENTAL PROGRAM**

### 2.1 Test Variables and Materials

The test variables, as shown in Table 1, include three water-to-binder ratios (W/B; 0.25, 0.35, 0.40) and three cement replacement ratios each for silica fume (RSF; 5%, 10%, 15%) and fly ash (RFA; 10%, 20%, 30%), respectively. The materials used for concrete mixture include an ordinary Type I Portland cement, natural sand, coarse aggregate, silica fume, fly ash, and a polycarboxylate based superplasticizer (SP) conforming to ASTM C494 Type G. The sand has a specific gravity of 2.69 and fineness modulus of 3.09. The coarse aggregate is crushed sandstone with a maximal nominal size of 12.7 mm and specific gravity of 2.60. The river silica fume has a specific gravity of 2.21 and an activity index at 7 day of 94.4%. The fly ash was obtained from a power station in central Taiwan. It was classified as low-calcium class F fly ash. The concrete was mixed according to the specification of ACI 211.2. A unified target slump of 150mm was selected for all concrete mixtures. Table 2 lists the mixture proportions of the concrete.

Table 1 Test factors and variables

Factors	Variables		
Water binder ratio (W/B)	0.25	0.35	0.40
Cement replacement ratio of silica fume	5%	10%	15%
Cement replacement ratio of fly ash	10%	20%	30%

Table 2 Mixture proportions of HSC (kg/m<sup>3</sup>)

Mixture	air(%)	W/B	Water	Cement	RSF	RFA	Fine aggregate	Coarse aggregate						
W25-S05-F10	2.0	0.25	146	510	30	60	497	1138						
W25-S05-F20				450		120	572	1043						
W25-S05-F30				390		180	645	950						
W25-S10-F10				2.0	0.25	146	480	60	60	576	1050			
W25-S10-F20							420		120	650	956			
W25-S10-F30							360		180	481	1101			
W25-S15-F10							2.0	0.25	146	450	90	60	654	963
W25-S15-F20										390		120	484	1108
W25-S15-F30										330		180	557	1015
W35-S05-F10	2.0	0.35	148							365	21	43	544	1244
W35-S05-F20										322		86	629	1145
W35-S05-F30										279		129	712	1048
W35-S10-F10				2.0	0.35	148	343	43	43	631	1150			
W35-S10-F20							300		86	715	1053			
W35-S10-F30							257		129	532	1218			
W35-S15-F10							147	322	43	718	1057			
W35-S15-F20								279	86	534	1222			
W35-S15-F30								236	129	617	1125			
W40-S05-F10	2.0	0.4	148	319	19	38	558	1278						
W40-S05-F20				281		75	647	1178						

W40-S05-F30			244		113	733	1079
W40-S10-F10			300	38	38	649	1182
W40-S10-F20			263		75	736	1083
W40-S10-F30			225		113	548	1254
W40-S15-F10		147	281	56	38	738	1087
W40-S15-F20			244		75	550	1258
W40-S15-F30			206		113	637	1160

## 2.2 Fabrication of Specimens

The slab specimens with a dimension of 600 mm × 600 mm × 100 mm was cast using a steel plate mould. Thermistor (Fig. 1) was embedded in the specimens for measuring the interior temperature development. Eight thermistors were placed in each specimen, as shown in Fig. 2. At the center section of specimen, Nos. 1, 2 and 8 were set vertically in the bottom, middle and top layers, respectively, while No. 2, 3, 4, 5, 6 and 7 ran counterclockwise, setting horizontally at the middle layer of the specimen. When the HSC mixture was ready prepared, it was poured in two layers into the mould while following the compaction for each half layer. After casting the specimens were stored in a curing room with a temperature of 23°C and a relative humidity of 50%. The specimens were left in the moulds throughout the whole measuring process.



Fig. 1 Thermistors

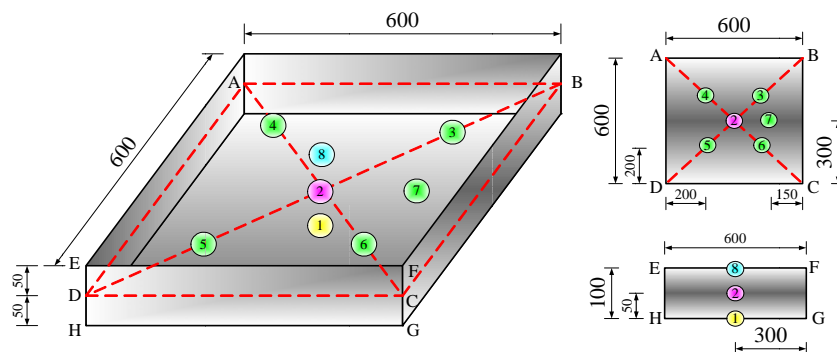


Fig. 2 Location of embedded thermistors in specimen

## 2.3 Temperature Measurement and Crack Detection

The interior temperature of the slab specimens was measured using the thermally sensitive resistors (or thermistors). A self-developed system, thermally sensitive detecting circuitry, was adopted to continuously measure the internal temperature change of the specimens. The thermistor possesses a resistance-temperature characteristic that its interior resistance varies with the change of temperature. The temperature was measured immediately after casting until 4 days.

Besides the temperature measurement, a parallel test for the surface cracking of specimens at early age was carried out with a high-resolution digital camera to monitor the occurred cracking of the specimens. The specimens were tested for 4 days. During the test, the crack was observed in the pictures at 5 x magnification. The time to the first appearance of cracking is called the cracking time. The total length and area of the surface crack are then analyzed to investigate the influence of temperature changes on the surface crack at early age.

### **3. RESULTS AND DISCUSSION**

#### *3.1 Interior Temperature Distribution of HSC Slab at Early Age*

The chronological development of interior temperature of the slab specimens was carefully observed and recorded throughout the test. All specimens exhibited similar temperature change and interior temperature distributions. The measured results of specimen W35-S10-F20 presented in **Fig. 3**, as an example, can be used to interpret the temperature change immediately after casting and up to an age of 4 days. In this period five stages can be divided as follows:

1. Initial temperature dropping down stage: From 1 to 6 hours the temperature in the specimen rises to a peak and sharply declines similar for all the 8 thermistors. In this stage, the concrete is in a plastic state, and is weak in strength that the surface cracking may occur.
2. Temperature rising stage: From 6 to 18 hours, the interior temperature of the specimen rapidly increases. The middle layer presents higher temperature than those of the top and bottom layers. The thermal will be transmitted from the middle to the outer part, forming a temperature gradient. The induced thermal deformation may lead to initial microcracking or surface cracking at this stage.
3. Second temperature dropping down stage: Between 18 and 24 hours, the temperature of the specimen decreases rapidly because the rate of hydration gets declining. At this stage, the concrete reaches to the final set, and strength gain increases gradually. Nevertheless, the temperature differences may induce the tensile stress in concrete. This will cause cracking, when the induced tensile stress exceeds the due strength of the concrete.
4. Slow temperature descending stage: From 24 to 96 hours (1 to 4 days), the temperature of specimen continues to decrease gradually until a steady state is reached.

- Steady temperature stage: After 4 days, the interior temperature of the specimen reaches to the ambient temperature. This is a steady state of no more temperature change in the concrete.

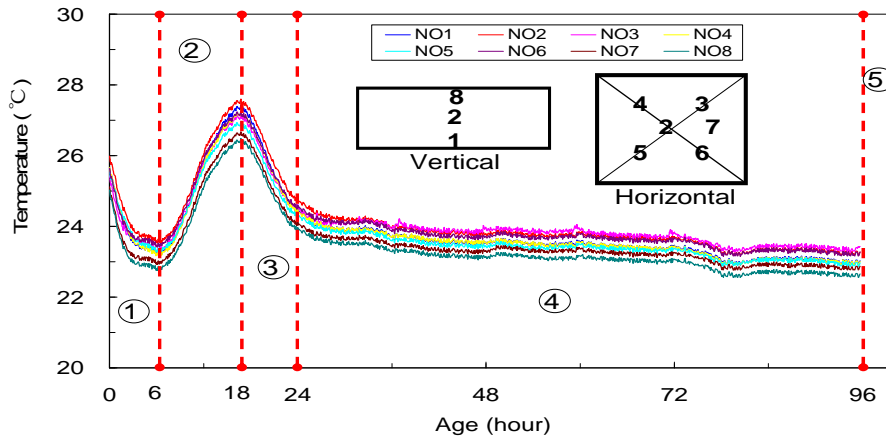


**Fig. 3** Temperature development of specimen W35-S10-F20 measured from 8 thermistors

### 3.1.1 Vertical Temperature Distribution

The vertical temperature variation in the specimens was measured by the thermistors No. 1, 2 and 8. Table 3 lists the measured temperature results at the top, middle and bottom layer of vertical direction for the specimens with various water-to-binder ratio (W/B), cement replacement ratio of silica fume (RSF) and fly ash (RFA). The temperature at middle layer consistently presents the highest value. As an example, Fig. 4 shows the vertical temperature development of the specimen W35-S10-F20. The middle layer (No. 2) presents the highest temperature for all ages, followed by bottom layer (No. 1), the top layer (No. 8) is the lowest. After 96 hours, the bottom and top layer approach to the ambient temperature due to heat exchange, while the middle layer reaches a steady state.

As stated previously, the temperature development in the HSC slab at early age is mainly influenced by the binder materials and the heat-storing ability. According to the characteristics demonstrated at the second temperature dropping downs stage, it is suggested that the curing of HSC should begin 18 hours after placement, continuing at least for 4 days to prevent the occurrence of an excessive temperature gradient during this stage.

Table 3 Measured vertical temperature distribution of HSC slabs

W/B	RSF (%)	RFA (%)	Bottom layer (°C)	Middle layer (°C)	Top layer (°C)
0.25	5	10	30.2	30.6	29.5
		20	26.8	29	24.8
		30	24.8	27.7	23.9

	10	10	31.2	31.8	30.6
		20	27.9	29.3	27.7
		30	26.1	28.8	25.3
	15	10	35.3	37.3	34.6
		20	34.5	34.8	33.9
		30	28.1	30.3	26.3
0.35	5	10	28.9	28.8	28.4
		20	26.8	27.2	26.1
		30	25.9	26	24.9
	10	10	29.1	31.2	28.6
		20	27.4	27.6	26.5
		30	26.7	26.9	25.4
	15	10	34.2	35.7	33.8
		20	31.6	33.9	29
		30	27.9	29.7	25.4
0.40	5	10	28.3	27.4	26.7
		20	24.7	25.8	24.3
		30	23.7	25.1	23.5
	10	10	27.7	28.4	27.2
		20	26.0	27.1	24.9
		30	24.9	25.5	24.1
	15	10	29.1	30.3	28.9
		20	26.8	28.4	25.1
		30	25.8	27.3	24.0

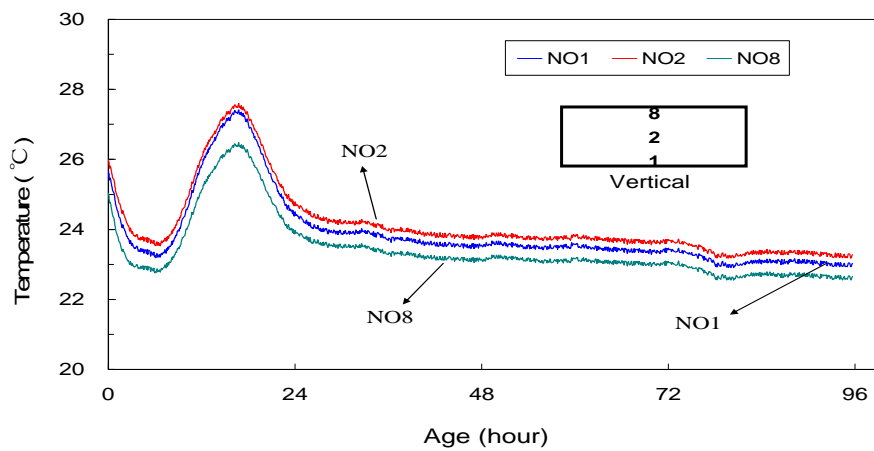


Fig. 4 Temperature distribution in vertical direction for specimen W35-S10-F20

### 3.1.2 Horizontal Temperature Distribution

The temperature variation of the specimens in horizontal direction was obtained from the thermistor No. 2 through No. 7. These thermistors recorded a similar temperature development. For example, the horizontal temperature development of specimen W35-S10-F20, as displayed in Fig. 5, shows that the temperature distribution in horizontal direction is similar to that in vertical direction. The temperature at No. 2, which locates at the center of the specimen, presents the highest value for all ages, followed by the temperatures of No. 3, 4, 5 and 6. No. 7, which is close to the outside edge of the steel mould, has the lowest temperature. These results imply that the central point of specimen exhibits the highest temperature. This temperature will be reduced gradually with distance away from the center to the outside edge.

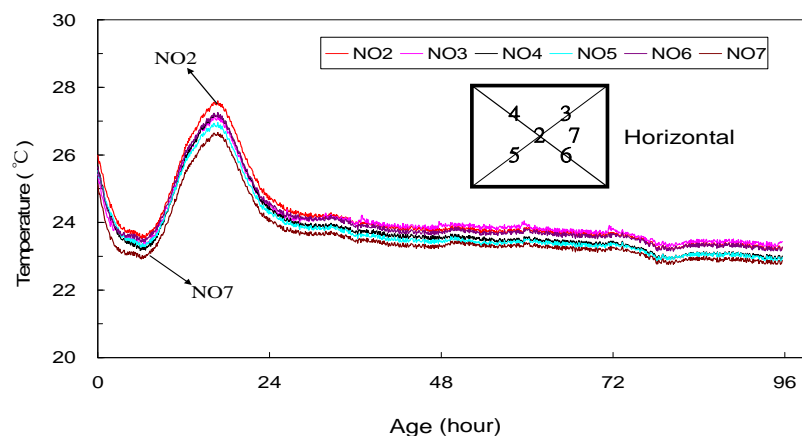


Fig. 5 Temperature distribution in horizontal direction for specimen W35-S10-F20

### 3.2 Influence of W/B on the Interior Temperature Development of HSC Slab

The hydration reaction of cement is exothermic and is accompanied by releases of heat. This heat will raise the temperature of the concrete. As soon as the cement first mixed with water, a period of rapid evolution of heat occurs, leading to the completion of the first heat peak in 10 to 15 minutes. Going through the induction period, when the silicate continues to hydrate rapidly and reaches a maximum rate of reaction at the end of acceleration period, which corresponds with the maximum rate of heat evolution that refers as second heat peak as shown by Mindess et al. (2003). Based on these heat characteristics of concrete, the temperatures at the central point of specimens were measured with thermistor No. 2 to evaluate the influence of W/B on the temperature development of HSC slab.

Fig. 6 plots the temperature development at the center of the specimens W25-S05-F30, W35-S05-F30 and W40-S05-F30. It is seen that the temperature of the initial or first heat peak of specimen W25-S05-F30 with lower W/B (0.25) is in turn higher than

those of the specimens W35-S05-F30 with higher W/B (0.35) and W40-S05-F30 (0.45). This implies that reducing the W/B ratio of HSC will enhance the temperature of the first heat peak. In the Fig. 6, it is also observed that the delayed second peak of the specimens appears more than 10 hours after casting. As mentioned previously, the second heat peak is related to the renewed reaction of the cement components ( $C_3S$  and  $C_3A$ ). The rate of this renewed hydration is slower than that of the initial peak hydration, so the second heat peak involved period presents to be wider and the reaction spans a longer period. Table 4 summarizes the measured results of the appearance time or the due time of second heat peak and the maximum temperature at the center of the specimens with various W/B and replacement ratios of silica fume and fly ash. It is found that the appearance time of the second peak has no quite definite relationship with the W/B, but shows a tendency to decrease with the decreases of W/B, whereas the maximum temperature increase obviously with the decrease of W/B. This can be also observed from Fig. 7 that for each series of the specimens with various RSF and RFA ratio, the peak temperature of the specimen decreases as W/B increase. In addition, since the appearance time of second heat peak corresponds to the final set as presented by Mehta (1986), it can be concluded that the increase of W/B increases the time of final set.

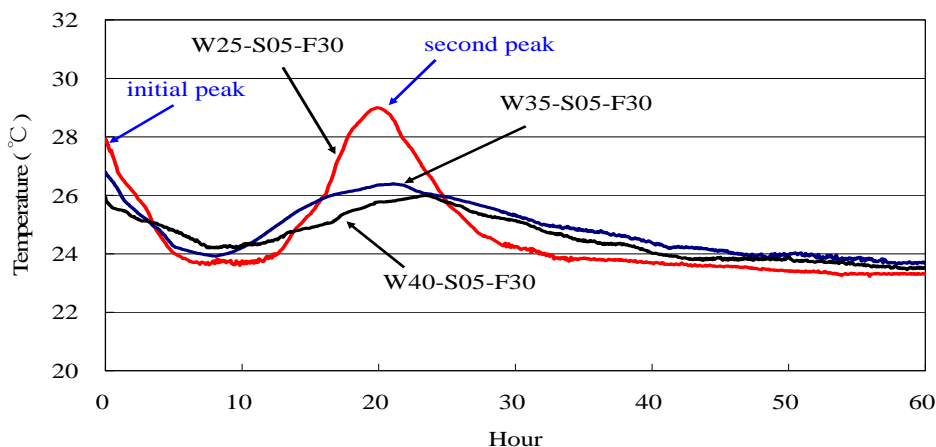


**Fig. 6** Temperature development at the center of specimen with different W/B

**Table 4** Measured appearance time and peak temperature of second heat peak at the center of specimens

W/B	RSF (%)	RFA (%)	appearance time (hr)	maximum temperature (°C)
0.25	5	10	17.1	30.6
		20	19.5	29.0
		30	23.6	27.7
	10	10	13.8	31.8
		20	15.8	29.3
		30	17.5	28.8

	15	10	10.3	37.3
		20	15.4	34.8
		30	15.8	30.3
0.35	5	10	20.1	28.8
		20	20.8	27.2
		30	23.4	26.0
	10	10	16.8	31.2
		20	17.3	27.6
		30	20.8	26.9
	15	10	18.1	35.7
		20	18.3	33.9
		30	22.2	29.7
0.40	5	10	15.4	27.4
		20	20.1	25.8
		30	21.1	25.1
	10	10	15.5	28.4
		20	17.1	27.1
		30	20.5	25.5
	15	10	19.2	30.3
		20	20.2	28.4
		30	20.5	27.3

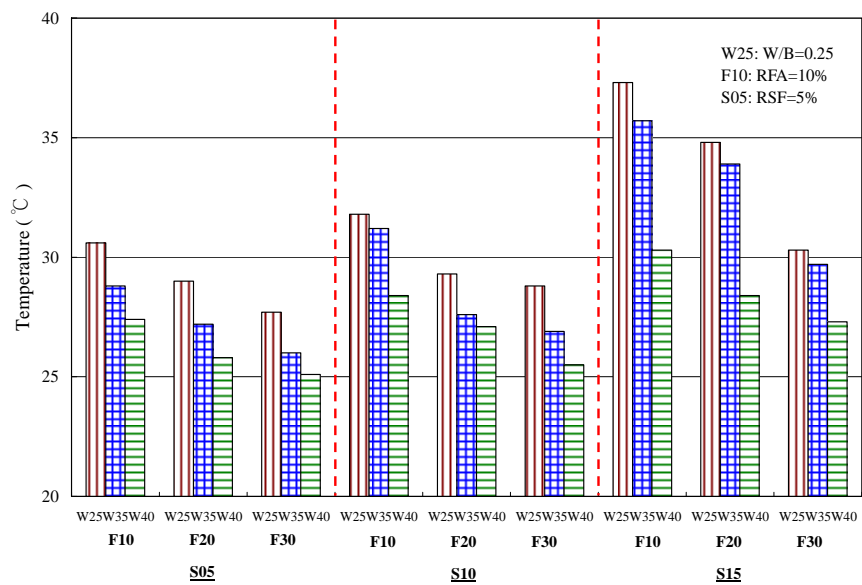


Fig. 7 Relations between maximum central temperature of specimens and the W/B ratio

### 3.3 Influence of Mineral Material on the Interior Temperature Development of HSC Slab

Comparing the appearance time of the second heat peak for the specimens with various mineral replacement ratio (RSF and RFA), it is found from Table 4 that the appearance time basically decrease with the increase of RSF, but increase with the increase of RFA for various W/B.

Fig. 8 shows the relations between maximum central temperature of specimen and the RSF. It is seen that for constant W/B and RFA, the maximum temperature may enhance when the RSF increases. On the other hand, as shown in Fig. 9, the maximum central temperature of specimen decreases with the increase of RFA for constant W/B and RSF.

The previous results imply the facts that incorporation of various silica fume and fly ash in HSC may affect the temperature development of the specimen. Increase the RSF may decrease the appearance time of second heat peak and increase the maximum central temperature of specimen, whereas, increase the RFA will increase the appearance time of second peak and decrease the maximum central temperature of specimen.

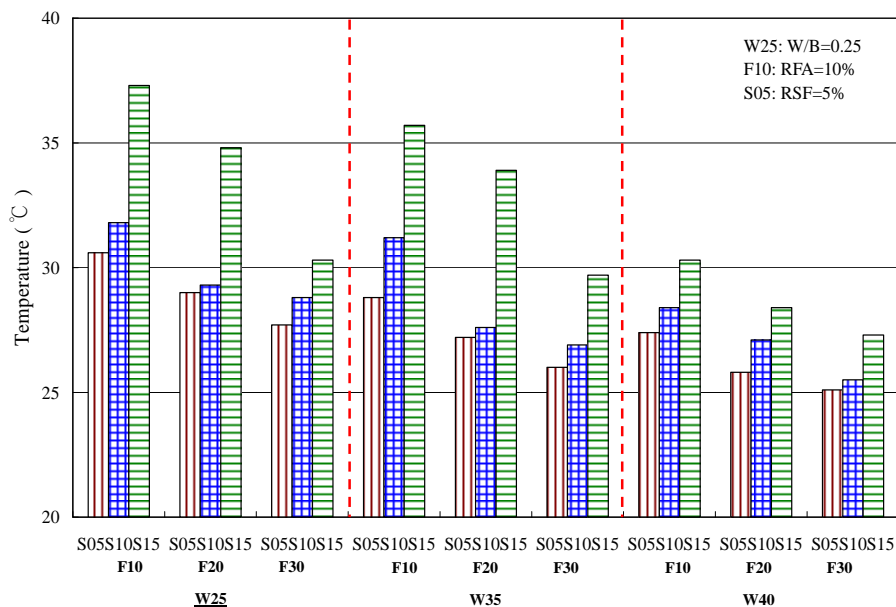


Fig. 8 Relations between maximum central temperature of specimens and the RSF ratio

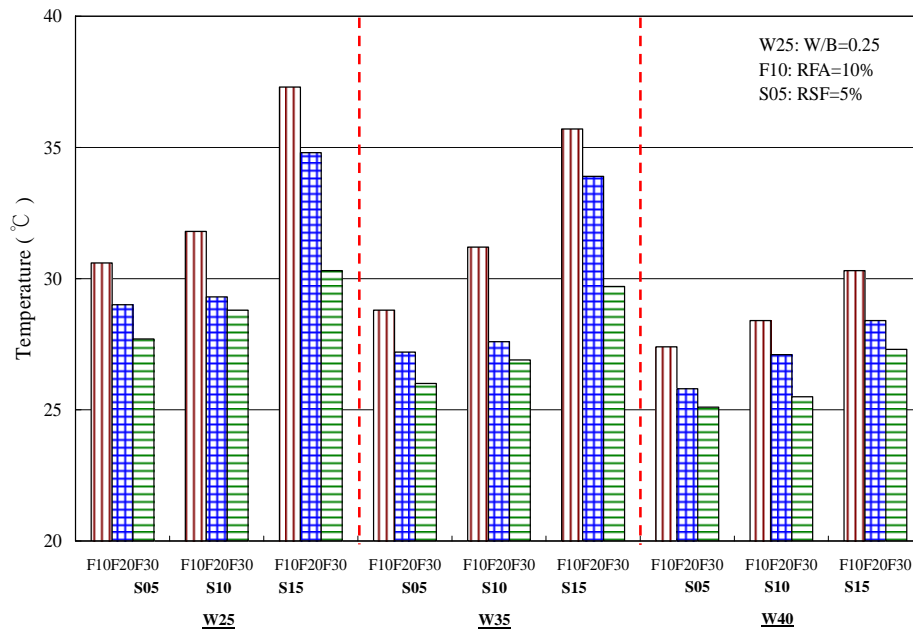


Fig. 9 Relations between maximum central temperature of specimens and the W/B ratio

### 3.4 Early Age Cracking of HSC Slab with Various RSF and RFA

Hydration reaction of cement and binder release heat of hydration that may induce the thermal expansion of concrete. Cracking due to thermal expansion is caused by tensile stresses that are created by differential strain that occur under temperature rise. So the thermal cracking resembles a linear flexural cracking as described by Mindess (2003).

In this investigation, a high-resolution digital camera is adopted to observe and measure the cracks occurred on the surface of specimen. Table 5 shows the occurrence time of cracking for all specimens. The specimens with W/B of 0.25 are cracked within 1 hour after casting, within 1 to 3 hours for W/B of 0.35, and within 2 to 4 hours for W/B of 0.40. This implies that the HSC slab with W/B of 0.25 to 0.40 may induce cracking within 4 hours after casting. Accordingly, it is suggested to make an appropriate curing during this period.

Table 5 Occurring time of surface crack on the specimens of HSC slab

W/B	RSF (%)	RFA (%)	crack occurring time (hr)
0.25	5	10	1
		20	1
		30	1
	10	10	0.5
		20	1

		30	1
	15	10	0.5
		20	1
		30	1
0.35	5	10	2
		20	3
		30	3
	10	10	1.5
		20	2.5
		30	3
	15	10	1
		20	2
		30	2.5
0.4	5	10	3.5
		20	4
		30	4
	10	10	3
		20	3.5
		30	4
	15	10	2
		20	3
		30	4

In the experiments, the length and maximum width of crack were adopted for evaluating the cracking intensity of the specimens. Table 6 shows the measured results of cracking characteristics for the specimens with different W/B. It is seen that the specimen with lower W/B of 0.25 (W25-S15-F10) exhibits in turn larger crack width, more crack length and crack number than those of specimens W35-S15-F10 and W40-S15-F10. The significance of these results is in accordance with the results shown in Table 4 that specimen W25-S15-F10 presents the least appearance time of second heat peak and highest maximum temperature among the three specimen series. In additional, the total crack length of the specimen series of W25 with various RSF and RFA are summarized in Table 7. It is observed that the total crack length for each comparison series of specimens displayed as follows: for similar RFA, total crack length of W25-S05-F10 < W25-S10-F10 < W25-S15-F10; for similar RSF, total crack length of W25-S05-F10 > W25-S05-F20 > W25-S05-F30. As a whole, the slab made of HSC incorporating some amount of silica fume and fly ash, when the W/B ranges between 0.25 and 0.40, is apt to crack. Reducing W/B may lead to intensive crack damage on slab, such as more crack number and larger crack with and length. The increase of

RSF increases the total crack length on the slab, whereas increase of RFA decreases the total crack length.

Table 6 Cracking characteristics of specimens with various W/B within 4 days

Mixture	W/B	RSF (%)	RFA (%)	Max. width (mm)	Crack number	Total crack length (mm)
W25-S15-F10	0.25	15	10	0.22	73	1533
W35-S15-F10	0.35			0.18	28	2171
W40-S15-F10	0.40			0.08	25	889

Table 7 Measured crack length of specimen series W25 within 1 hour

Mixture	W/B	RSF (%)	RFA (%)	Total length (mm)
W25-S05-F10	0.25	5	10	35
W25-S05-F20			20	11
W25-S05-F30			30	6
W25-S10-F10		10	10	83
W25-S10-F20			20	49
W25-S10-F30			30	44
W25-S15-F10		15	10	94
W25-S15-F20			20	61
W25-S15-F30			30	52

#### 4. CONCLUSIONS

Slab specimens were cast with HSC incorporating silica fume and fly ash and embedded with thermistors to investigate the interior temperature development of HSC slab. The test results support the following conclusions:

1. The interior temperature development of HSC slabs at early age can be divided into five stages - initial temperature dropping down stage, temperature rising stage, second temperature dropping down stage, slow temperature descending stage and steady temperature stage.
2. In the vertical direction of the central section of specimens, the temperature at the middle layer is the highest for all ages, followed by that of bottom layer, the top layer shows the lowest temperature.
3. The central point of the specimen in the horizontal direction exhibits the highest temperature. This temperature will be gradually reduced with the distance away from the center to the outside edge.
4. Reducing the W/B ratio of HSC will enhance the temperature of the first heat peak by hydration. The decrease of W/B decreases the appearance time of the second heat peak, but increases the maximum central temperature of slab.
5. Increase the RSF of HSC may decrease the appearance time of second heat

- peak and increase the maximum central temperature of slab.
6. Increase the RFA of HSC will increase the appearance time of second heat peak and decrease the maximum central temperature of slab.
  7. The HSC slab with the range of W/B of 0.25 to 0.40 may occur cracking within 4 hours after casting. Slab with lower W/B exhibits larger crack width, more crack length and crack number.
  8. The increase of RSF increases the total crack length on the slab, whereas increases of RFA decrease the total crack length.

## ACKNOWLEDGEMENTS

The authors appreciate the Taiwan Power Company for financially support of this research under Contract No. 601-4412.

## REFERENCES

- Mehta, P.K. (1986), "Concrete. Strength, properties and materials," Prentice-Hall, Inc. Englewood Cliffs, N.J., pp. 187-191.
- Zou, X., Chao, A., Tian, Y., Wu, N., Zhang, H., Yu, T.Y. and Wang, X. (2012) "An experimental study on the concrete hydration process using Fabry-Perot fiber optic temperature sensors," *Measurement*, **45**, 1077-1082.
- Chu, I., Lee, Y., Amin, M.N., Jang, B.S. and Kim, J.K. (2013) "Application of a thermal stress device for the prediction of stresses due to hydration heat in mass concrete structure," *Construction and Building Materials* **45**, 192-198.
- Mindess, S., Young, J.F. and Darwin, D. (2002), Concrete, second edition, 417-418.
- Li, G.D., Wang, Z.L. and Zhao, W.P. (2016), "Early-age autogenous shrinkage and stress characteristics of high-performance concrete at the mesoscopic level," *Magazine of Concrete Research*, **68**(16), 809-822.
- ACI Committee 363 (2010), "State-of-the-Art Report on High-Strength Concrete – ACI 363R," USA
- Bentz, D.P. (2008), "A Review of Early-Age Properties of Cement-Based Materials," *Cement Concrete Research*, **38**(2), 196-204.
- Langan B.W., Weng K. and Ward M.A. (2002), "Effect of silica fume and fly ash on heat of hydration of Portland cement," *Cement and Concrete Research*, **32**(7), 1045-1051.
- Utsi, S. and Jonasson, J.E. (2012), "Estimation of the risk for early thermal cracking for SCC containing fly ash," *Materials and Structures*, **45**(1-2), 153-169.
- Jiang C.H., Yang Y., Ni T. and Wang X.D. (2015), "Correlating strength of concrete to its early-age temperature rise," *Magazine of Concrete Research*, **67**(23), 1274-1286.
- Maria, K. (2002), "Early age properties of high-strength/high-performance concrete", *Cement and Concrete Composites*, **24**(2), 253-261.
- Yang, Y.A., Sato, R. and Kawai, K. (2005), "Autogenous shrinkage of high-strength concrete containing silica fume under drying at early ages," *Cement and Concrete Research*, **35**(3), 449-456.
- Holt E. and Leivo M. (2004), "Cracking risks associated with early age shrinkage," *Cement and Concrete Composites*, **26**, 521-530.
- Yoo D.Y., Min K.H., Lee J.H. and Yoon Y.S. (2014), "Shrinkage and cracking of restrained ultra-high-performance fiber-reinforced concrete slabs at early age," *Construction and Building Materials*, **73**, 357-365.
- Mindess S., Young J. F. and Darwin D. (2003), "Concrete," second edition, Parson Education, Inc. N. J., 57-65.

- Wan L., Wendner R., Liang B. and Cusatis G. (2016), "Analysis of the behavior of ultra high performance concrete at early age," *Cement and Concrete Composites*, **74**, 120-135.
- Mihashi, H., and Leite, J.P. (2004). "State of the art report on control of cracking in early age concrete," *J. Advanced Concrete Technology*, **2**(2), 141-154.
- Al-Fadhala M. and Hover K.C. (2001), "Rapid evaporation from freshly cast concrete and the Gulf environment," *Cement and Building Material*, **15**, 1-7.
- Huo X.S. and Wong L.U. (2006), "Experimental study of early-age behavior of high performance concrete deck slabs under different curing methods," *Cement and Building Material*, **20**(10), 1049-1056.
- Park J.S., Kim Y.J., Cho J.R. and Jeon S.J. (2015), "Early-age strength of ultra-high performance concrete in various curing conditions," *Materials*, **8**(8), 5537-5553.
- Lin, F., Song, X.B., Gu, X.L., Peng, B. and Yang, L.P. (2012), "Cracking analysis of massive concrete walls with cracking control techniques," *Construction and Building Material*, **31**, 12-21.